

Classification of endometrial adenocarcinoma using histopathology images with extreme learning machine method

Riries Rulaningtyas¹, Anny Setijo Rahaju^{2,3,4}, Rosa Amalia Dewi¹, Ummi Hanifah⁵, Endah Purwanti¹, Osmalina Nur Rahma¹, Katherine⁵

¹Biomedical Engineering Study Program, Department of Physics, Faculty of Science and Technology, Universitas Airlangga, Surabaya, Indonesia

²Department of Anatomical Pathology, Faculty of Medicine, Universitas Airlangga, Surabaya, Indonesia

³Department of Anatomical Pathology, Dr. Soetomo General Academic Hospital, Surabaya, Indonesia

⁴Department of Anatomical Pathology, Universitas Airlangga Hospital, Surabaya, Indonesia

⁵Master of Biomedical Engineering Study Program, Department of Physics, Faculty of Science and Technology, Universitas Airlangga, Surabaya, Indonesia

Article Info

Article history:

Received Dec 9, 2023

Revised Jun 25, 2024

Accepted Jul 14, 2024

Keywords:

Endometrial adenocarcinoma

Extreme learning machine

Gray level run length matrix

Histopathology images

Local binary pattern

ABSTRACT

As many as 70-80% of endometrial cancer cases are endometrial adenocarcinoma. Histopathological assessment is based on the degree of differentiation, into well-differentiated, moderate-differentiated, and poorly-differentiated. Management and prognosis differ between grades, so differential diagnosis in determining the degree of tumor differentiation is crucial for appropriate treatment decisions. Histopathological image analysis offers detailed diagnostic results, but manual analysis by a pathologist is very complicated, error-prone, quite tedious, and time-consuming. Therefore, an automatic diagnostic system is needed to assist pathologists in grading the tumor. This research aims to determine the degree of differentiation of endometrial adenocarcinoma based on histopathological images. The extreme learning machine (ELM) method performs image classification with gray level run long matrix (GLRLM) features and a combination of local binary pattern (LBP)-GLRLM features as input. Experimental results show that the ELM model can achieve satisfactory performance. Training accuracy, testing accuracy, and model precision with GLRLM features were 97.13%, 91.33%, and 80% and combined LBP-GLRLM features were 91.03%, 71.33%, and 100%. Overall, the model created can determine the degree of tumor differentiation and is useful in providing a second opinion for pathologists.

This is an open access article under the [CC BY-SA](https://creativecommons.org/licenses/by-sa/4.0/) license.



Corresponding Author:

Riries Rulaningtyas

Biomedical Engineering Study Program, Department of Physics, Faculty of Science and Technology

Universitas Airlangga

Surabaya, Indonesia

Email: riries-r@fst.unair.ac.id

1. INTRODUCTION

Endometrial cancer is the sixth most common gynecological tumor and its prevalence is increasing. It is the 14th leading cause of cancer deaths in women worldwide, but is often diagnosed at stage 1 due to its symptomatic nature [1], [2]. Endometrial carcinoma is classified by histological type, including endometrioid carcinoma (EEC), serous carcinoma (SC), clear cell carcinoma (CCC), mixed carcinoma (MC), undifferentiated carcinoma (UC), carcinosarcoma (CS), gastrointestinal mucinous type carcinomas, and other types [3]. Endometrial adenocarcinoma is a type of EEC that arises due to excessive exposure to estrogen

with risk factors including obesity, anovulation, nulliparity, and administration of exogenous estrogen [1]. As many as 70-80% of endometrial carcinoma cases show endometrioid features with varying degrees of differentiation and metaplastic changes [4], [5].

Histopathological classification based on tumor morphology and tumor grade has played an important role in the management of endometrial carcinoma [6]. The degree of differentiation is one of the important prognostic factors of histopathologic assessment, which is divided into well-differentiated (grade 1), moderate-differentiated (grade 2), and poorly-differentiated (grade 3). Low-grade EEC (grade 1 or 2) belongs to the non-aggressive histological subtype. Development is relatively slow after prolonged estrogenic stimulation [3], [7]. In contrast, high-grade EEC (grade 3) belongs to an aggressive histological subtype, has a worse prognosis with a high growth pattern of non-glandular solid masses, and tends to spread beyond the uterine structure. This tumor type is heterogeneous prognostically, clinically, and molecularly and thus is the one that benefits most from the application of molecular classification [3], [7], [8]. The 5-year specific survival in high-grade EEC is significantly lower than in low-grade due to more frequent metastases and a higher risk of recurrence [9]. Management and prognosis between subtypes also differ, so differential diagnosis is very important for appropriate treatment decisions [6], [9]–[11]. Determination of the histological subtype by a pathologist is carried out by examining tissue sample slides stained with hematoxylin and eosin from tumor samples [5], [12]. This analysis offers detailed diagnostic results, but its visualization is not always exclusive to subtypes because some morphological features overlap, making histological classification difficult even for experienced pathologists [5], [7], [10]. Manual analysis by pathologists is very complicated, more prone to errors, quite tedious, and time-consuming [13]. Thus, an automated diagnostic system is needed to assist pathologists in distinguishing the degree of EEC differentiation from a large number of medical images efficiently.

In recent years, the development of artificial intelligence has enabled the use of advanced approaches in the health sector, while increasing diagnostic accuracy and providing second opinions in diagnostic procedures [14]–[16]. Previous research shows that artificial intelligence can be applied in the classification of various types of cancer, such as the subtype classification of ovarian carcinoma [14], endometrial cancer [11], and breast cancer [12], [17]–[19]. In the case of endometrial cancer, previous studies focused on predicting histological subtypes between EEC and SC types. Prediction of EEC and SC histological subtypes in endometrial cancer using the InceptionResnet-based multi-resolution convolutional neural network (CNN) architecture, Panoptes, resulted in an area under the receiver operating characteristic (AUROC) of 0.969 with a confidence level of 95%. The images used in this research are digital histopathological images cut into small tiles and colored with H&E staining. The model created can process as many as 22 sets of tiles per second within 4 minutes, which means it can work simultaneously with a pathologist for reference [5]. Our main interest is to classify histopathological images to determine the degree of differentiation of the endometrioid type in endometrial cancer. Hyperastuty *et al.* [12] determined the degree of differentiation for breast cancer using the artificial neural network (ANN) method. Backpropagation training on histopathological images with 10 hidden layer neurons produces 81.1% accuracy and 80% precision. Other researchers used a tiered approach of support vector machine (SVM) classifiers with a combination of features to classify breast cancer grade and produced an overall accuracy of 69% [20]. However, according to our knowledge, this differentiation degree approach has never been used in previous studies for endometrial adenocarcinoma cases.

In this study, we used the extreme machine learning (ELM) method to determine the degree of differentiation of endometrial adenocarcinoma. ELM was chosen because of its ability to detect complex trends with good generalization performance at a very fast learning rate [21]. The application of ELM in cancer classification has been carried out in several studies. Toprak's research on breast cancer classification in [19] resulted in a performance accuracy of 98.99% using the ELM method with 9 input features from histopathological images, better than SVM (96.85%) and Naïve-Bayes (95.99%). ELM was also used in the classification of normal and precancerous tissue in cervical cancer, resulting in model sensitivity and specificity of 94.6% and 84.3% [21]. Other researchers use it for the classification of brain tumors [22], skin cancer [23], and breast cancer [17], [24]. Feature extraction is carried out to improve ELM performance. Microscopic images can provide better information on texture features. Textural features represent the characteristic appearance of an object's surface which is associated with the size, shape, arrangement, and depth of its constituent elements [25]. Several feature extraction methods combined with ELM classification were compared in the research of Kumar *et al.* [22], the gray-level run length matrix (GLRLM) method produced sensitivity, specificity, and accuracy of 90%, 78%, and 84% respectively, better than the gray level co-occurrence matrix (GLCM) 81%, 65%, and 73%. Thus, we chose GLRLM as the feature extraction method in this study. Then we also apply the combined local binary pattern (LBP)-GLRLM feature. Combining texture features with a classifier can produce quite good accuracy. The classification results using the combined LBP-GLRLM feature extraction method are better than LBP or GLRLM alone, with an accuracy rate of 98.41% [26]. In this

combined method, the endometrial adenocarcinoma image that has gone through the grayscaling process is feature extracted using LBP to produce decimal numbers, then reconstructed back into an image for GLRLM feature retrieval.

The main purpose of this study was to develop an efficient machine learning model to automatically classify the degree of differentiation of endometrial adenocarcinoma into three subtypes from histopathological images taken using the biopsy method. The various stages carried out in this research include data collection, pre-processing, feature extraction, and classification. The contributions we made in this manuscript are summarized as follows: i) provide a machine learning-based model for automatic diagnosis based on the degree of differentiation of histopathological images of endometrial adenocarcinoma, ii) generate the best ELM model configuration in improving the classification performance of the degree of differentiation of endometrial adenocarcinoma, and iii) comparison of methods GLRLM extraction and combined LBP-GLRLM method in classifying the degree of differentiation using ELM.

2. METHOD

Our study focused on determining the degree of differentiation of endometrial adenocarcinoma which consists of three grades, namely well-differentiated (grade 1), moderate-differentiated (grade 2), and poorly-differentiated (grade 3). The procedures we followed to conduct this study are described below respectively. Figure 1 illustrates the procedural steps performed.

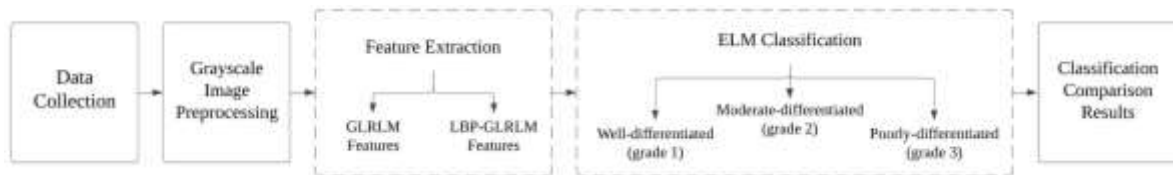


Figure 1. Block diagram of endometrial adenocarcinoma classification

2.1. Data collection

Data were collected at the Department of Anatomical Pathology of Dr. Soetomo Hospital Surabaya. The data obtained were histopathology images of grade 1, grade 2, and grade 3 endometrial adenocarcinoma differentiation degrees. Each grade contains 50 data with dimensions of 1440×1024. Histopathology images were obtained by biopsy method and then observed by digital microscope at 200× magnification with Hematoxilin-Eosin staining.

2.2. Pre-processing

Digital images are representations of intensity functions in a two-dimensional plane. Images can be grouped into three types based on their color, namely RGB, grayscale, and binary images. RGB images are composed of three color channels, red, green, and blue. While grayscale and binary images only have one color channel. In RGB and grayscale images, the intensity value of pixels with 8-bit depth varies between 0 and 255. The difference with binary images, the depth is 1-bit, so the color intensity is only expressed by the value 0 means black and 1 means white [12]. In this study, the image obtained is an RGB image so it is necessary to do grayscaling or convert the RGB image to grayscale. The goal is to improve image quality so as to facilitate the feature extraction stage and reduce computational burden. Another reason the grayscaling process is needed is because the selected feature extraction method only analyzes the gray level in the image. Figure 2 shows the results of image preprocessing from RGB to grayscale images. Preprocessing of endometrial adenocarcinoma images from RGB images to grayscale can be seen in Figure 2(a) for grade 1 adenocarcinoma, in Figure 2(b) for grade 2 adenocarcinoma, and in Figure 2(c) for grade 3 adenocarcinoma. RGB images are converted to grayscale using the (1).

$$Gray = (0.299 \times R) + (0.587 \times G) + (0.144 \times B) \tag{1}$$

2.3. Feature extraction

To sort out the relevant characteristics that characterize each class, we perform feature extraction. Machine learning-based image classification requires feature extraction first to increase accuracy. For microscopic images, texture features can provide better information. This feature represents the characteristic appearance of an object's surface which is associated with the size, shape, arrangement, and depth of its

constituent elements [25]. Combining texture features with a classifier can produce quite good accuracy [26]. We use two feature extraction methods in this research, namely gray level run length matrix (GLRLM) and combined LBP–GLRLM. Features from both methods have been used as machine learning input and have shown good performance [22], [26].

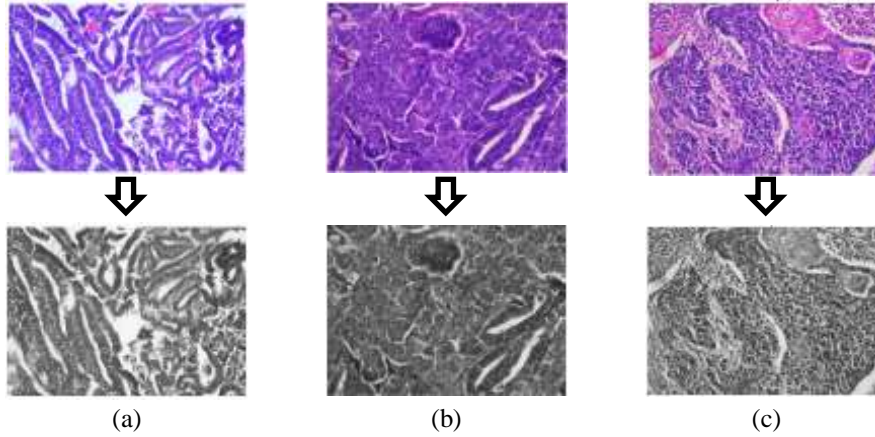


Figure 2. Preprocessing results of endometrial adenocarcinoma histopathology images: (a) grade 1, (b) grade 2, and (c) grade 3

2.3.1. Gray level run length matrix

GLRLM extracts the gray degrees present in the grayscale image. The extraction begins with determining the angle orientation, which is 0, 45, 90, and 135, then forming a run-length matrix at each angle. An angle of 0 means horizontal direction, i.e. the pixel is compared to the pixel on the right. An angle of 90 means the vertical direction, i.e. the pixel is compared to the pixel above it. An angle of 45 means a diagonal direction with a positive gradient, where the pixel is compared to the pixel to the right of it. A 135 angle means a diagonal direction with a positive gradient, where the pixel is compared to the pixel to the upper left. The use of four angular orientations can ease the computation process as there is no need to use multiple angular orientations. Figure 3 shows the run-length matrix results from image processing with four angle orientations.

The run-length matrix $p(i, j)$ is defined as the sum of run-length with gray-level pixels i and run-length j . Various texture features can be derived from the matrix [25]. The GLRLM features used are gray-level nonuniformity (GLN), run length nonuniformity (RLN), run percentage (RP), low gray-level run emphasis (LGRE), high gray-level run emphasis (HGRE/HGL), short run low gray-level emphasis (SRLGE), short run high gray-level emphasis (SRHGE), long run high gray-level emphasis (LRHGE). These eight features will be the input for the classification stage.

$$GLN = \frac{1}{n_r} \sum_{i=1}^M (\sum_{j=1}^N p(i, j))^2 = \frac{1}{n_r} \sum_{i=1}^M p_g(i)^2 \quad (2)$$

$$RLN = \frac{1}{n_r} \sum_{j=1}^M (\sum_{i=1}^N p(i, j))^2 = \frac{1}{n_r} \sum_{j=1}^M p_r(i)^2 \quad (3)$$

$$RP = \frac{n_r}{n_p} \quad (4)$$

$$LGRE = \frac{1}{n_r} \sum_{i=1}^M \sum_{j=1}^N \frac{p(i, j)}{i^2} = \frac{1}{n_r} \sum_{i=1}^M \frac{p_g(i)}{i^2} \quad (5)$$

$$HGRE = \frac{1}{n_r} \sum_{i=1}^M \sum_{j=1}^N p(i, j) \cdot i^2 = \frac{1}{n_r} \sum_{i=1}^M p_g(i) \cdot i^2 \quad (6)$$

$$SRLGE = \frac{1}{n_r} \sum_{i=1}^M \sum_{j=1}^N \frac{p(i, j)}{i^2 \cdot j^2} \quad (7)$$

$$SRHGE = \frac{1}{n_r} \sum_{i=1}^M \sum_{j=1}^N \frac{p(i, j) \cdot i^2}{j^2} \quad (8)$$

$$LRHGE = \frac{1}{n_r} \sum_{i=1}^M \sum_{j=1}^N p(i, j) \cdot i^2 \cdot j^2 \tag{9}$$

n_r is the total number of runs and n_p is the number of pixels in the image. GLN, RLN, and RP belong to traditional run-length features and most of the features are only a function of $p_r(j)$ without considering the gray-level information on $p_g(i)$. To extract the gray level information in the matrix, LGR and HGRE are used. Then there are combined statistical measures between gray level and run-length, namely SRLGR, SRHGR, and LRHGE are also used in this study.

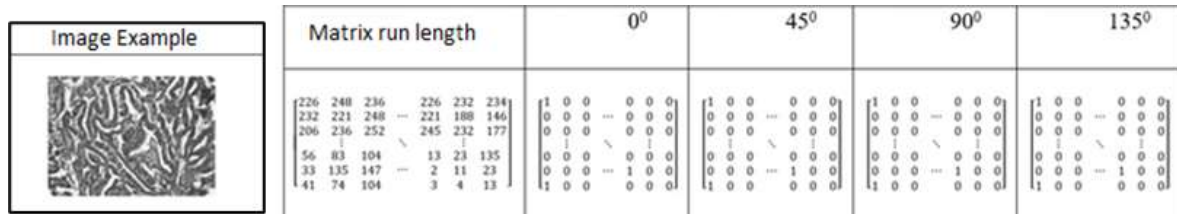


Figure 3. Matrix run length in each angular orientation

2.3.2. Local binary pattern

LBP is a feature extraction method used for texture classification in image processing. LBP has become a very efficient texture feature descriptor. A 3×3 mask is used against neighboring pixels to determine a particular texture and evaluate the LBP. LBP is also said to be a first-order circular derivative of the micro-pattern contained in the image that can be constructed by conjugating all binary gradient directions. The mathematical model can be seen as (10).

$$LBP(P, R) = \sum_{p=0}^{P-1} s(q_p - q_c) 2^p \tag{10}$$

With P being the number of neighboring pixels, $s(x) = 0$ when $x > 0$ and 1 otherwise [26].

A combined LBP and GLRLM method is used in this research. The output of the grayscaleing process will be feature extracted using LBP to produce decimal numbers based on the grayscale image. LBP works by comparing the binary value of the pixel at the center of the image with the value of its neighboring pixels, then the binary results are summed with weights. The result of LBP is reconstructed back into an image, then GLRLM features are extracted to obtain 8 types of texture features. The grayscale image and LBP reconstructed image are seen in Figure 4, along with the resulting array values. The array values of grade 1 endometrial adenocarcinoma from the grayscale image can be seen in Figure 4(a) and the array values of grade 1 endometrial adenocarcinoma from the LBP reconstructed image can be seen in Figure 4(b).

LBP produces a representation of the local values for each pixel. The LBP result image contains information about the local texture pattern in the original image. The difference between the grayscale image and the LBP image can be seen visually from the sharpness and texture of the image. The LBP image displays an image with a dot pattern that shows a variety of texture patterns in the image that looks sharper and more blur. Meanwhile, grayscale images can represent images with gray levels from low gray to high gray clearly. This is because the LBP image has been reconstructed and the pixel values have been processed so as to get the characteristic value of the image.

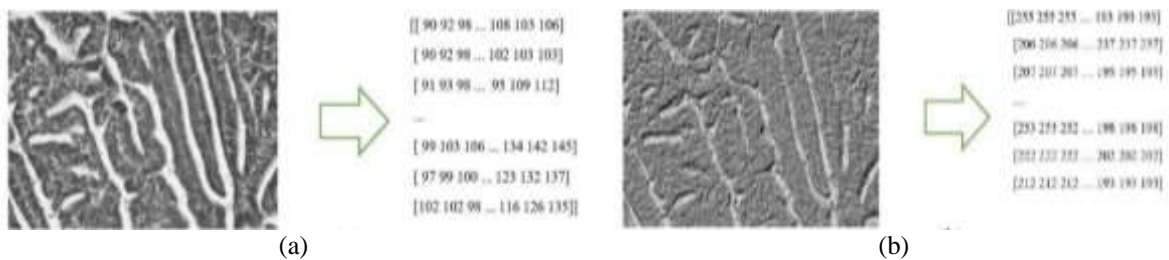


Figure 4. Array values of grade 1 endometrial adenocarcinoma from (a) grayscale image and (b) LBP reconstructed image

2.4. Extreme learning machine classification

ELM is a development of feedforward neural network method that has only one hidden layer, referred to as single hidden-layer neural network. This method has a learning speed thousands of times faster than traditional feedforward, and produces better generalization performance. Unlike FNNs that only tend to achieve the smallest error, ELM also achieves the smallest weight norm. In its learning, the output weights are calculated analytically, while the input weights are chosen randomly [19], [27]. Here is the architecture of ELM shown by Figure 5.

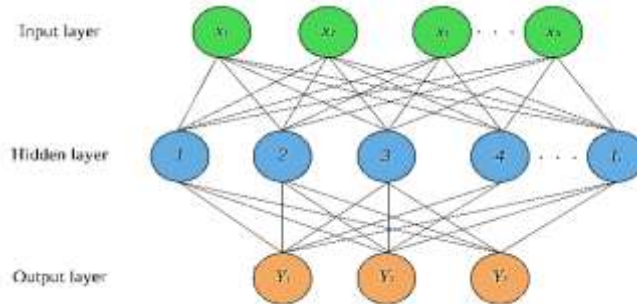


Figure 5. ELM architecture

Training ELM is to find the best weights w_i , bias b_i , and beta β_i . The algorithm starts by specifying the input x_i and target t_i . The input is an average representing each feature from the GLRLM or LBP-GLRLM feature extraction results and the output is three classes, namely grade 1, grade 2, and grade 3. Then the output Y_j of the ELM with N hidden neurons can be expressed into the (11):

$$\sum_{i=1}^N \beta_i g(w_i x_j + b_i) = Y_j, j = 1, \dots, N \tag{11}$$

With $g(x)$ is the activation function in the hidden layer. The equation can be simplified into the (12).

$$H\beta = Y \tag{12}$$

The weight and bias values are determined randomly, then the output of the hidden layer matrix H is calculated. The matrix H is of size $a \times b$, where a is the number of inputs and b is the number of hidden nodes. β can be obtained from (12) by using the Moore-Penrose inverse [27], [28]:

$$\beta = H^T Y \tag{13}$$

the matrix H can be written as (14) and (15).

$$H = \begin{bmatrix} g(w_1 x_1 + b_1) & \dots & g(w_N x_1 + b_N) \\ \vdots & \ddots & \vdots \\ g(w_1 x_N + b_1) & \dots & g(w_N x_N + b_N) \end{bmatrix} \tag{14}$$

$$\beta = \begin{bmatrix} \beta_1^T \\ \vdots \\ \beta_N^T \end{bmatrix}_{N \times m}, Y = \begin{bmatrix} y_1^T \\ \vdots \\ y_N^T \end{bmatrix}_{N \times m} \tag{15}$$

The available data set is divided into two subsets, for training and testing. With a training subset, the ELM classifier is trained to learn optimal parameter settings. The maximum number of hidden nodes used in this research is 100 nodes and the activation function is a binary sigmoid function to recognize non-linear data. Testing is carried out after ELM training to find out how well the model created performs. We divided the training data and test data in a ratio of 80:20. Different schemes are often used for performance evaluation, such as k-fold cross-validation or exit-one-out [29]. We used k-fold cross-validation to test different data schemas, with values of $k = 10$. The k-fold method divided the data set into train, validation, and test data along with splitting, mode selection, and performance states [19].

2.5. Performance metrics

Classification performance is measured quantitatively by training accuracy, testing accuracy, and precision derived from confusion matrix parameters: true positive, false positive, true negative, false negative. Table 1 is a confusion matrix used to measure multiclass classification performance. G1, G2, G3 are the differentiation degree of endometrial adenocarcinoma grade 1, grade 2, and grade 3, respectively. GG1, GG2, and GG3 are the number of actual G1, G2, G3 classes that are predicted correctly in their respective classes. While the other 6 values are the number of actual G1, G2, or G3 classes that are predicted incorrectly in each classified column.

Table 1. Confusion matrix

		Predicted result		
		G1	G2	G3
Actual result	G1	GG1	G1G2	G1G3
	G2	G2G1	GG2	G2G3
	G3	G3G1	G3G2	GG3

Accuracy is a value that will be used to measure the accuracy of a detection or classification system. The accuracy value is measured as the ratio between the data that can be guessed correctly by the algorithm and the total of all data. If the accuracy of a detection system is high then the system can perform the detection process well, otherwise if the accuracy of a detection system is low then the system is said to be unable to perform the detection process properly. Meanwhile, precision is the proportion of correctly classified images to the total of all predictions/diagnoses of correctly detected images [19]. The following is the equation for the level of accuracy and precision, where *N* is total amount of data.

$$\text{Accuracy} = \frac{GG1+GG2+GG3}{N} \tag{16}$$

$$\text{Precision GG1} = \frac{GG1}{G1G2+G1G3} \tag{17}$$

$$\text{Precision GG2} = \frac{GG2}{G2G1+G2G3} \tag{18}$$

$$\text{Precision GG3} = \frac{GG3}{G3G1+G3G2} \tag{19}$$

3. RESULTS AND DISCUSSION

Endometrial adenocarcinoma is divided into three classes according to the degree of differentiation. Each grade has different characteristics but is difficult to identify with the naked eye. Grade 1 is characterized by the glands still being visible and the cells arranged neatly resembling normal cells, grade 2 having irregular glands and cells arranged in a pile, and grade 3 not seeing the glands and the cells are becoming more condensed and denser. There are two ELM models produced in this research, which are divided based on the feature extraction method carried out before classification. The model1 was created using feature extraction input using the GLRLM method and the model2 used feature extraction input using the combined LBP-GLRLM method. The LBP method produces decimal numbers from grayscale images. The results from LBP are then reconstructed into images to be extracted using the GLRLM feature. The results of feature extraction each amount to 8 types of GLRLM texture features from four angular orientations, and then the average is calculated to represent each feature. Normalization is carried out using the MinMax scaler method before the ELM process so that the processed data has the same scale. Data processing is carried out using Python programming.

The proposed classification of the degree of differentiation of endometrial adenocarcinoma was assessed using evaluation metrics of accuracy and precision. The differentiation degree classification results are shown in Table 2. ELM can achieve the lowest error rate and output weight norm values in one iteration, making this model faster than gradient-based learning algorithms. The performance of the ELM model depends on the initialization of the weights, the number of nodes in the hidden layer, and the type of activation function [24]. We use the K-fold cross-validation data segmentation method to find the best ELM model configuration. The k-fold method can separate data sets, select models, and test performance [19]. In this process, the best number of hidden nodes was 40 in the model1 and 82 in the model2. We determine the maximum number of nodes in the hidden layer to be 100. The activation function we use is the binary sigmoid function because this function can recognize non-linear data. The accuracy graph of the ELM

models can be seen in Figure 6. The accuracy graph of ELM with GLRLM feature (model1) has been illustrated in Figure 6(a) and the accuracy graph of the ELM with LBP-GLRLM feature (model2) has been illustrated in Figure 6(b). It can be seen that the accuracy increases around the number of best hidden ones, then decreases. ELM shows the best performance for training accuracy of 97.13%, testing accuracy of 91.33%, and precision of 80% on the model1. Meanwhile, training accuracy was 91.03%, testing accuracy was 71.33%, and precision was 100% in the model2. The metric results are evaluated in percentages as they indicate the effectiveness of the classifier. High accuracy indicates precise and accurate tumor classification with lower false negatives. The high-precision results demonstrate the correctness of the proposed algorithm. The performance of the ELM model1 shows better results than the model2. This is because the extracted input image has significant differences in characteristics between each class in pure GLRLM features, in contrast to the GLRLM input from LBP results where the range of feature values is not much different between each class. Other research shows that the combination of LBP-GLRLM features produces quite good values [26], but apparently, it depends on the image used.

Table 2. ELM classification results with GLRLM features

Feature extraction method	Best hidden nodes	Accuration (%)		Precision (%)
		Training	Testing	
GLRLM	40	97.13	91.33	80
LBP-GLRLM	82	91.03	71.33	100

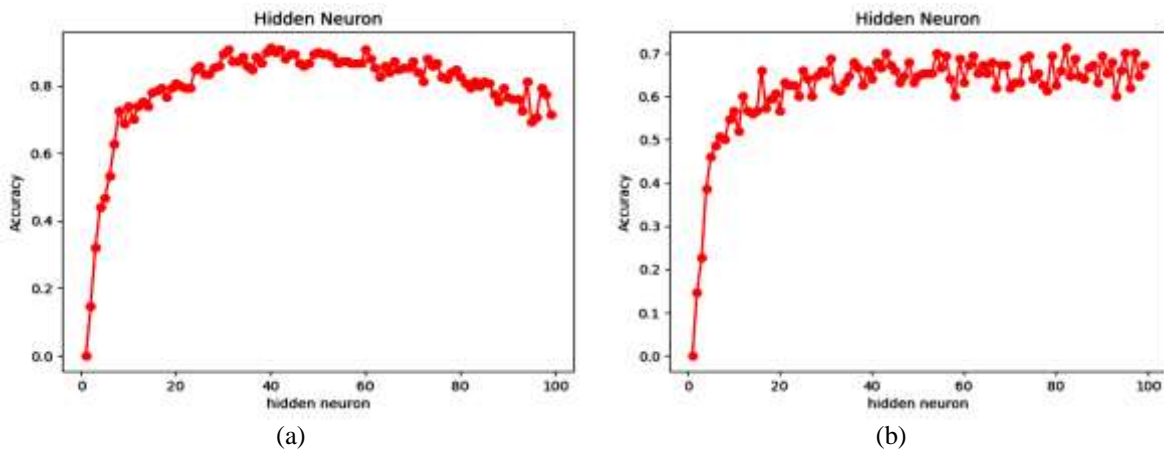


Figure 6. Accuracy graph of the (a) ELM with GLRLM feature and (b) ELM with LBP-GLRLM feature

The performance of the proposed ELM model in differentiation degree classification is compared with other machine learning methods. It can be seen in Table 3, there is a comparative analysis of the ELM classifier with other machine learning classifiers which have the same goal, that is the classification of the degree of tumor differentiation. Comparative analysis was taken from breast cancer and ovarian cancer where the cancer has a morphological structure similar to endometrial adenocarcinoma. The comparative studies presented all used histopathological images taken by biopsy and hematoxylin-eosin staining. The classifiers used for comparative analysis of endometrial adenocarcinoma classification are multiple SVM [20], you only look once (YOLO) with various versions [30], and CNN with Inception-V3 architecture [31]. The metrics used for performance evaluation are testing accuracy and precision. The ELM method with GLRLM features (model1) in this study shows higher performance than the presented comparative method. The testing accuracy obtained by ELM model1 was 91.33%, greater than the accuracy of other classifiers, which are 69% for SVM, 89% for YOLO-V3, 88% for Tiny-YOLO, 84% for YOLO-V2, 84% for YOLO-V1, 85% for CNN, and 71.33% for ELM models. The ELM method with LBP-GLRLM feature (model2) produce the lowest performance accuracy among other methods but have the highest precision, which is 100%, greater than the accuracy of other classifiers, which are 87% for YOLO-V3, 85% for Tiny-YOLO, 80% for YOLO-V2, 77% for YOLO-V1, and 80% for ELM model1. Thus, the proposed method can be used as a consideration for pathologists in increasing the accuracy of diagnosis of endometrial adenocarcinoma based on the degree of differentiation.

Table 3. Comparison of similar studies

Classification method	Classification object	Testing accuracy (%)	Precision (%)
Multiple SVM [20]	Grades of breast cancer	69	-
YOLO-V3 [30]	Grades of breast cancer	89	87
Tiny-YOLO [30]	Grades of breast cancer	88	85
YOLO-V2 [30]	Grades of breast cancer	84	80
YOLO-V1 [30]	Grades of breast cancer	81	77
Inception V3 CNN [31]	Grades of ovarian cancer	85	-
Proposed model 1	Grades of Adenokarsinoma endometrium	91.33	80
Proposed model 2	Grades of Adenokarsinoma endometrium	71.33	100

4. CONCLUSION

Prognostic determination of endometrial adenocarcinoma based on the degree of differentiation is carried out by processing histopathological images using the ELM classification method. Two different feature extraction methods, namely GLRLM and combined LBP-GLRLM, are used as input to the ELM classifier and produce different classification performances. The ELM model can classify the degree of differentiation into well-differentiated (grade 1), moderate-differentiated (grade 2), and poorly-differentiated (grade 3) with levels of training accuracy, testing accuracy, and precision are 97.13%, 91.33%, 80% for GLRLM features and 91.03%, 71.33%, 100% for combined LBP-GLRLM features. Increased accuracy and precision in the classification of endometrial adenocarcinoma are beneficial in the early management of the disease and can be used as a second opinion for pathologists.

ACKNOWLEDGEMENTS

This work was supported by DRTPM – Direktorat Jenderal Pendidikan Tinggi Kementerian Pendidikan dan Kebudayaan Republik Indonesia, with grant number (114/E5/PG.02.00.PL/2023 and 1312/UN3.LPPM/PT.01.03/2023).





REFERENCES

- [1] J. Lortet-Tieulent, J. Ferlay, F. Bray, and A. Jemal, "International patterns and trends in endometrial cancer incidence, 1978-2013," *Journal of the National Cancer Institute*, vol. 110, no. 4, pp. 354–361, 2018, doi: 10.1093/jnci/djx214.
- [2] P. Morice, A. Leary, C. Creutzberg, N. Abu-Rustum, and E. Darai, "Endometrial cancer," *The Lancet*, vol. 387, no. 10023, pp. 1094–1108, 2016, doi: 10.1016/S0140-6736(15)00130-0.
- [3] J. S. Berek *et al.*, "FIGO staging of endometrial cancer: 2023," *Journal of gynecologic oncology*, vol. 34, no. 5, p. e85, 2023, doi: 10.3802/jgo.2023.34.e85.
- [4] A. Azueta, S. Gatius, and X. Matias-Guiu, "Endometrioid carcinoma of the endometrium: pathologic and molecular features," *Seminars in Diagnostic Pathology*, vol. 27, no. 4, pp. 226–240, 2010, doi: 10.1053/j.semdp.2010.09.001.
- [5] R. Hong, W. Liu, D. DeLair, N. Razavian, and D. Fenyő, "Predicting endometrial cancer subtypes and molecular features from histopathology images using multi-resolution deep learning models," *Cell Reports Medicine*, vol. 2, no. 9, 2021, doi: 10.1016/j.xcrm.2021.100400.
- [6] A. Santoro *et al.*, "New pathological and clinical insights in endometrial cancer in view of the updated esgo/estro/esp guidelines," *Cancers*, vol. 13, no. 11, pp. 1–20, 2021, doi: 10.3390/cancers13112623.
- [7] G. F. Zannoni *et al.*, "Does high-grade endometrioid carcinoma (grade 3 FIGO) belong to type I or type II endometrial cancer? A clinical-pathological and immunohistochemical study," *Virchows Archiv*, vol. 457, no. 1, pp. 27–34, 2010, doi: 10.1007/s00428-010-0939-z.
- [8] A. Bermudez, N. Bhatla, and E. Leung, "Cancer of the cervix uteri," *International Journal of Gynecology and Obstetrics*, vol. 131, pp. S88–S95, 2015, doi: 10.1016/j.ijgo.2015.06.004.
- [9] G. Khatib, U. K. Gulec, A. B. Guzel, E. Bagir, S. Paydas, and M. A. Vardar, "Prognosis trend of grade 2 endometrioid endometrial carcinoma: toward grade 1 or 3?," *Pathology and Oncology Research*, vol. 26, no. 4, pp. 2351–2356, 2020, doi: 10.1007/s12253-020-00836-w.
- [10] J. Y. Song, S. Im, S. H. Lee, and H. J. Jang, "Deep learning-based classification of uterine cervical and endometrial cancer subtypes from whole-slide histopathology images," *Diagnostics*, vol. 12, no. 11, 2022, doi: 10.3390/diagnostics12112623.
- [11] H. Sun, X. Zeng, T. Xu, G. Peng, and Y. Ma, "Computer-aided diagnosis in histopathological images of the endometrium using a convolutional neural network and attention mechanisms," *IEEE Journal of Biomedical and Health Informatics*, vol. 24, no. 6, pp. 1664–1676, 2020, doi: 10.1109/JBHI.2019.2944977.
- [12] A. S. Hyperastuty, A. S. R. Setijo, and R. R., "Artificial neural network in determining histopathological grading of breast cancer [Translation] (in Indonesian: *Artificial neural network dalam menentukan grading histopatologi kanker payudara*)" *Jurnal Biosains Pascasarjana*, vol. 19, no. 2, p. 176, 2017, doi: 10.20473/jbp.v19i2.2017.176-188.
- [13] K. V. Deepak and R. Bharanidharan, "Osteosarcoma detection in histopathology images using ensemble machine learning techniques," *Biomedical Signal Processing and Control*, vol. 86, no. PC, p. 105281, 2023, doi: 10.1016/j.bspc.2023.105281.
- [14] A. Bentaieb, M. S. Nosrati, H. Li-Chang, D. Huntsman, and G. Hamameh, "Clinically-inspired automatic classification of ovarian carcinoma subtypes," *Journal of Pathology Informatics*, vol. 7, no. 1, p. 28, 2016, doi: 10.4103/2153-3539.186899.
- [15] M. Chen, Y. Hao, K. Hwang, L. Wang, and L. Wang, "Disease prediction by machine learning over big data from healthcare communities," *IEEE Access*, vol. 5, pp. 8869–8879, 2017, doi: 10.1109/ACCESS.2017.2694446.
- [16] M. Wu, C. Yan, H. Liu, and Q. Liu, "Automatic classification of ovarian cancer types from cytological images using deep convolutional neural networks," *Bioscience Reports*, vol. 38, no. 3, pp. 1–7, 2018, doi: 10.1042/BSR20180289.





- [17] H. D. Bizuneh, S. Mishra, and W. G. Negassa, "Breast tumor detection and classification using ABC-ELM algorithm," *2023 International Conference in Advances in Power, Signal, and Information Technology, APSIT 2023*, pp. 81–85, 2023, doi: 10.1109/APSIT58554.2023.10201776.
- [18] S. Lyu and R. C. C. Cheung, "Efficient and automatic breast cancer early diagnosis system based on the hierarchical extreme learning machine," *Sensors*, vol. 23, no. 18, p. 7772, 2023, doi: 10.3390/s23187772.
- [19] A. Toprak, "Extreme learning machine (ELM)-based classification of benign and malignant cells in breast cancer," *Medical Science Monitor*, vol. 24, pp. 6537–6543, 2018, doi: 10.12659/MSM.910520.
- [20] T. Wan, J. Cao, J. Chen, and Z. Qin, "Automated grading of breast cancer histopathology using cascaded ensemble with combination of multi-level image features," *Neurocomputing*, vol. 229, pp. 34–44, 2017, doi: 10.1016/j.neucom.2016.05.084.
- [21] J. Gu, C. Y. Fu, B. K. Ng, L. B. Liu, S. K. Lim-Tan, and C. G. L. Lee, "Enhancement of early cervical cancer diagnosis with epithelial layer analysis of fluorescence lifetime images," *PLoS ONE*, vol. 10, no. 5, pp. 1–15, 2015, doi: 10.1371/journal.pone.0125706.
- [22] K. Kavin Kumar, T. Meera Devi, and S. Maheswaran, "An efficient method for brain tumor detection using texture features and SVM classifier in MR images," *Asian Pacific Journal of Cancer Prevention*, vol. 19, no. 10, pp. 2789–2794, 2018, doi: 10.22034/APJCP.2018.19.10.2789.
- [23] D. Jayalakshmi and J. Dheebea, "Computer aided diagnostic support system for skin cancer using ELM classifier," *International Journal of System Assurance Engineering and Management*, vol. 15, no. 1, pp. 449–461, 2022, doi: 10.1007/s13198-022-01775-2.
- [24] D. Muduli, R. R. Kumar, J. Pradhan, and A. Kumar, "An empirical evaluation of extreme learning machine uncertainty quantification for automated breast cancer detection," *Neural Computing and Applications*, vol. 1, 2023, doi: 10.1007/s00521-023-08992-1.
- [25] X. Tang, "Texture information in run-length matrices," *IEEE Transactions on Image Processing*, vol. 7, no. 11, pp. 1602–1609, 1998, doi: 10.1109/83.725367.
- [26] S. Das and U. R. Jena, "Texture classification using combination of LBP and GLRLM features along with KNN and multiclass SVM classification," *2nd International Conference on Communication, Control and Intelligent Systems, CCIS 2016*, pp. 115–119, 2017, doi: 10.1109/CCIS2016.7878212.
- [27] G. Bin Huang, Q. Y. Zhu, and C. K. Siew, "Extreme learning machine: theory and applications," *Neurocomputing*, vol. 70, no. 1–3, pp. 489–501, 2006, doi: 10.1016/j.neucom.2005.12.126.
- [28] J. Wang, S. Lu, S.-H. Wang, and Y.-D. Zhang, "A review on extreme learning machine," *Multimedia-Based Healthcare Systems Using Computational Intelligence*, vol. 81, pp. 41611–41660, 2022, doi: 10.1007/978-3-031-21452-3_2.
- [29] L. He, L. R. Long, S. Antani, and G. R. Thoma, "Histology image analysis for carcinoma detection and grading," *Computer Methods and Programs in Biomedicine*, vol. 107, no. 3, pp. 538–556, 2012, doi: 10.1016/j.cmpb.2011.12.007.
- [30] S. M. and J. Joy, "A machine learning based framework for assisting pathologists in grading and counting of breast cancer cells," *ICT Express*, vol. 7, no. 4, pp. 440–444, 2021, doi: 10.1016/j.icte.2021.02.005.
- [31] Y. Liu, B. C. Lawson, X. Huang, B. M. Broom, and J. N. Weinstein, "Prediction of ovarian cancer response to therapy based on deep learning analysis of histopathology images," *Cancers*, vol. 15, pp. 2588–2593, 2023, doi: 10.3390/cancers15164044.

BIOGRAPHIES OF AUTHORS






Riries Rulaningtyas     received the Bachelor of Engineering and Master of Engineering in Electrical Engineering from Institut Teknologi Sepuluh Nopember, Indonesia and a Doctor of Engineering in Electrical Engineering from Bandung Institute of Technology, Indonesia. Currently, she is a lecturer at the Biomedical Engineering Study Program, the Department of Physics, Faculty of Science of Technology, Universitas Airlangga, Indonesia. Her research interests include biomedical image and signal processing, machine learning and artificial intelligence. She can be contacted at email: riries-r@fst.unair.ac.id.






Anny Setijo Rahaju     received the Bachelor of Medicine, Specialist of Anatomical Pathology, and Doctor of Medicine from Faculty of Medicine Universitas Airlangga, Indonesia. Her research interests include anatomical pathology, pediatric gastroenterology, immunology, and microbiota. She can be contacted at email: anny_sr@fk.unair.ac.id.






Rosa Amalia Dewi    received the Bachelor of Engineering in Biomedical Engineering from Universitas Airlangga, Indonesia in 2023. Her research interests include biomedical image and artificial intelligence. She can be contacted at email: rosa.amaliadewii@gmail.com.






Ummi Hanifah    received the Bachelor of Engineering in Biomedical Engineering from Airlangga University, Indonesia, in 2023 and currently became a master student in biomedical engineering from Universitas Airlangga. Her research interests include biomedical instrumentation and artificial intelligence. She can be contacted at email: ummi.hanifah-2023@fst.unair.ac.id.






Endah Purwati    received the Bachelor of Science in Physics from Universitas Airlangga, Indonesia, in 2001 and the Master of Engineering from Institut Teknologi Sepuluh Nopember, Indonesia, in 2009. Currently, she is a lecturer at the Biomedical Engineering Study Program, the Department of Physics, Faculty of Science of Technology, Universitas Airlangga, Indonesia. Her research interests include biomedical image processing, signal processing and artificial intelligence. She can be contacted at email: Endah-p-1@fst.unair.ac.id.



Osmalina Nur Rahma    received the Bachelor of Engineering in Biomedical Engineering from Universitas Airlangga, Indonesia, in 2013 and the Master of Science in Biomedical Engineering from the University of Indonesia, Indonesia, in 2016. Currently, she is a lecturer at the Biomedical Engineering Study Program, the Department of Physics, Faculty of Science of Technology, Universitas Airlangga, Indonesia. Her research interests include biomedical instrumentation, image and signal processing, and rehabilitation engineering. She can be contacted at email: osmalina.n.rahma@fst.unair.ac.id.



Katherine    received the Bachelor of Engineering in Biomedical Engineering from Universitas Airlangga, Indonesia, in 2020 and the Bachelor of Engineering in Biomedical Engineering from the Airlangga University, Indonesia, in 2024. Her research interests include biomedical image processing, biomedical signal processing and artificial intelligence. She can be contacted at email: katherine-2021@fst.unair.ac.id.